Title

Therapeutic effects of cell-permeant peptides that activate G proteins downstream of growth factors

Journal

Proceedings of the National Academy of Sciences of the United States of America, 112(20)

ISSN

0027-8424

Authors

S., Gary
Aznar, Nicolas
Kalogriopoulos, Nicholas
et al.

Publication Date

2015-05-19

DOI

10.1073/pnas.1505543112

Peer reviewed

Therapeutic effects of cell-permeant peptides that activate G proteins downstream of growth factors

Gary S. Ma[a,1], Nicolas Aznar[a,1], Nicholas Kalogriopoulos[a], Krishna K. Midde[a], Inmaculada Lopez-Sanchez[a], Emi Sato[a], Ying Dunkel[a], Richard L. Gallo[a,b], and Pradipta Ghosh[a,b,2]

[a]Department of Medicine, University of California, San Diego School of Medicine, La Jolla, CA 92093; and [b]Department of Veterans Affairs, VA San Diego Healthcare System, San Diego, CA 92161

Edited by Solomon H. Snyder, Johns Hopkins University School of Medicine, Baltimore, MD, and approved April 10, 2015 (received for review April 7, 2015)

In eukaryotes, receptor tyrosine kinases (RTKs) and trimeric G proteins are two major signaling hubs. Signal transduction via trimeric G proteins has long been believed to be triggered exclusively by G protein-coupled receptors (GPCRs). This paradigm has recently been challenged by several studies on a multimodular signal transducer, Gα-Interacting Vesicle associated protein (GIV/Girdin). We recently demonstrated that GIV's C terminus (CT) serves as a platform for dynamic association of ligand-activated RTKs with Gαi, and for noncanonical transactivation of G proteins. However, exogenous manipulation of this platform has remained beyond reach. Here we developed cell-permeable GIV-CT peptides by fusing a TAT-peptide transduction domain (TAT-PTD) to the minimal modular elements of GIV that are necessary and sufficient for activation of Gi downstream of RTKs, and used them to engineer signaling networks and alter cell behavior. In the presence of an intact GEF motif, TAT-GIV-CT peptides enhanced diverse processes in which GIV's GEF function has previously been implicated, e.g., 2D cell migration after scratch-wounding, invasion of cancer cells, and finally, myofibroblast activation and collagen production. Furthermore, topical application of TAT-GIV-CT peptides enhanced the complex, multireceptor-driven process of wound repair in mice in a GEF-dependent manner. Thus, TAT-GIV peptides provide a novel and versatile tool to manipulate Gαi activation downstream of growth factors in a diverse array of pathophysiologic conditions.

heterotrimeric G proteins | fibrosis | cell-permeable GIV/Girdin peptide | wound healing | invasion

Receptor Tyrosine Kinases (RTK) and G protein coupled receptors (GPCR) are the two most widely studied cell signaling hubs in eukaryotes. For several decades, these two pathways were believed to operate in discrete modes by transducing signals through their respective downstream intermediates; upon ligand stimulation, RTKs propagate the signals to the interior of the cell via adaptor proteins that are recruited to phosphotyrosines on the receptor tail (1), whereas GPCRs, which are 7-transmembrane (TM) receptors with an intrinsic Guanine nucleotide Exchange Factor (GEF) activity recruit and activate G proteins by triggering the exchange of GDP with GTP nucleotide (2). Gathering evidence over time has unraveled a complex cross-talk between these two pathways at multiple tiers (3, 4). For example, transactivation of RTKs by GPCRs via scaffolding proteins, such as β-arrestins (5), is a well documented and widely accepted phenomenon. Numerous studies have also provided evidence to support the reverse concept, i.e., transactivation of heterotrimeric G proteins by growth factors (6). However, it was not until recently that this concept gained traction with the discovery and characterization of Gα-Interacting Vesicle associated protein (GIV; a.k.a. Girdin), an unusual signal transducer that can bind both RTKs and G proteins.

GIV is a multimodular (Fig. 1*A*) signal transducer and a GEF for Gαi (7). Working downstream of a variety of growth factors [EGF (8, 9), IGF (10), VEGF (11), Insulin (7, 12, 13), and PDGFR (14)] GIV modulates (i.e., either enhances or suppresses) a variety of signaling pathways, all via its ability to activate Gαi in the close proximity of ligand-activated RTKs (7). Multiple studies (summarized in Fig. S1; ref. 15) using a selective GEF-deficient GIV mutant (F1685A) have demonstrated that the signaling network downstream of RTKs in cells with wild-type GIV is a mirror image of the network in cells expressing a GEF-deficient mutant GIV. It is because cells can alter (increase or decrease) the levels of GIV mRNA/protein or selectively modulate GIV's GEF activity to modulate growth factor signaling pathways across a range of intensities (16), we likened GIV to a cellular "rheostat" for signal transduction (17). Consistent with its ability to integrate signals downstream of multiple receptors, GIV modulates growth factor signaling during diverse biological processes (17), e.g., cell migration, chemotaxis (13), invasion (18), development (19), self-renewal (20), apoptosis (14, 21), and autophagy (12). Increasing evidence also supports the clinical significance of GIV-dependent signaling during diverse disease processes (17), e.g., pathologic angiogenesis (11), liver fibrosis (14), nephrotic syndrome (21), vascular repair (22), and tumor metastasis (23).

The molecular mechanisms that govern how GIV influences a diverse range of pathophysiologic processes and how it may couple activation of G protein to multiple receptors have come to light only recently, at least in the context of a numerous RTKs that signal via GIV. GIV-dependent growth factor signaling appears to rely heavily on the unique multimodular nature of its C terminus (CT), within which two unlikely domains coexist: (*i*) a previously defined GEF motif via which GIV binds and activates

Significance

Most common diseases (e.g., cancer, inflammatory disorders, diabetes) are driven by not one, but multiple cell surface receptors that trigger and sustain a pathologic signaling network. The largest fraction of therapeutic agents that target individual receptors/pathways often eventually fail due to the emergence of compensatory mechanisms. Recently, we identified GIV protein as a central platform for receptor cross-talk which integrates signals downstream of a myriad of upstream receptors, and modulates several key pathways within downstream signaling network, all via activation of trimeric G proteins. Here we provide the proof-of-concept that nongenetic exogenous modulation of the GIV-Gi signaling interface using cell-penetrable GIV-derived peptides is an effective strategy to reset pathologic signaling networks downstream of multiple receptors in a diverse array of pathophysiologic conditions.

Author contributions: G.S.M., N.A., N.K., K.K.M., I.L.-S., E.S., Y.D., R.L.G., and P.G. designed research; G.S.M., N.A., N.K., K.K.M., I.L.-S., E.S., and Y.D. performed research; R.L.G. and P.G. contributed new reagents/analytic tools; G.S.M., N.A., N.K., K.K.M., I.L.-S., E.S., Y.D., R.L.G., and P.G. analyzed data; and N.A., N.K., K.K.M., and P.G. wrote the paper.

The authors declare no conflict of interest.

This article is a PNAS Direct Submission.

[1]G.S.M. and N.A. contributed equally to this work.

[2]To whom correspondence should be addressed. Email: prghosh@ucsd.edu.

This article contains supporting information online at www.pnas.org/lookup/suppl/doi:10.1073/pnas.1505543112/-/DCSupplemental.

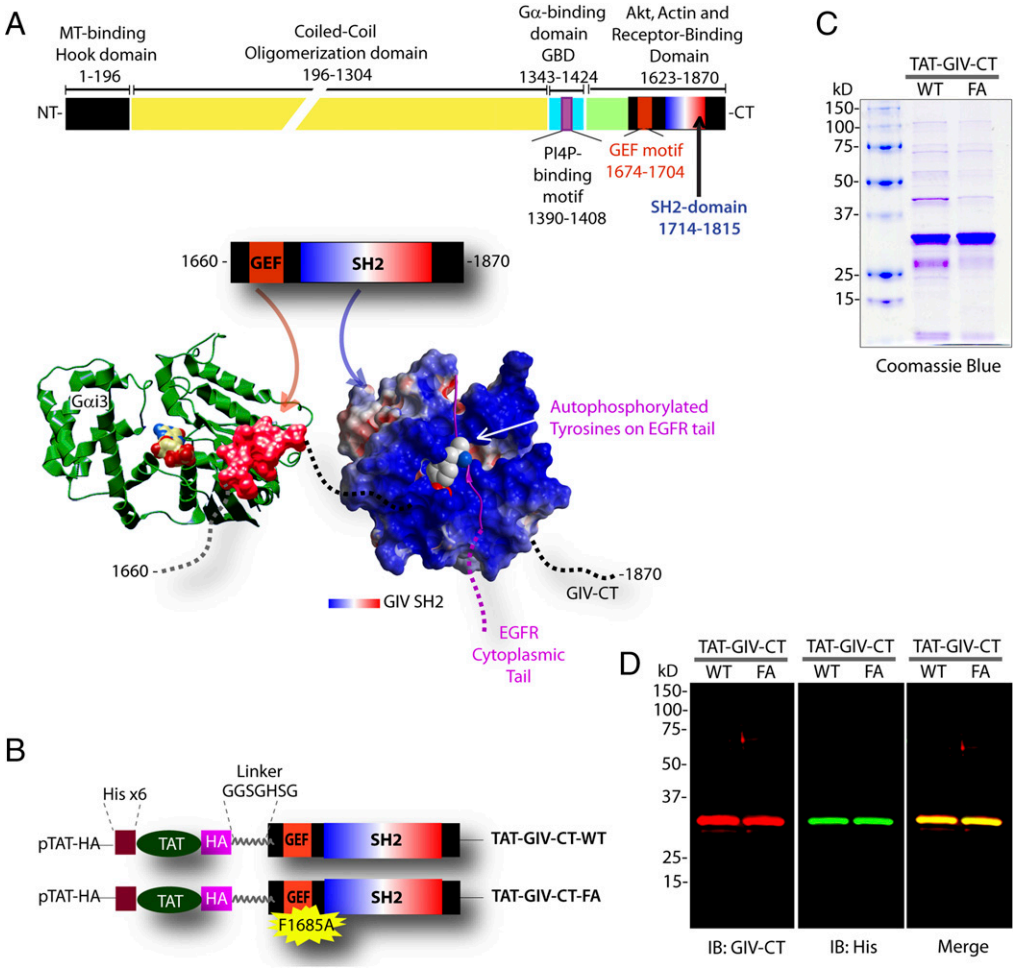

Fig. 1. Design and purification of cell-permeable TAT-GIV CT peptides. (*A*, *Upper*) Schematic representation of the domain organization of GIV. From left to right, the functional domains include a microtubule-binding hook domain (black), a coiled-coil homodimerization domain (yellow), a Gα-binding domain (GBD, blue), a phosphoinositide (PI4P) binding motif (purple), a GEF motif (red), and, finally, a SH2-like domain (red, white, and blue) that is located within the Akt and Actin-binding domains at the extreme C terminus. The numbers denote the amino acids marking the boundaries of each domain. (*A*, *Lower*) Schematic showing how GIV's C-terminal ∼210 amino acids link Gαi to the autophosphorylated cytoplasmic tail of ligand-activated RTKs. Homology model of Gαi3 in complex with GIV aa 1678–1689 (*Left*) was generated using the structure of the synthetic peptide KB-752 bound to Gαi1 (Protein Data Bank ID 1Y3A) as a template as done previously (7). Green, Gαi3 subunit; red, GIV's GEF motif. Model of GIV's SH2-like domain bound to a EGFR-derived phosphotyrosine peptide (purple) corresponding to pTyr1148 and its flanking residues is shown (*Right*) (30). The acidic, neutral, and basic potentials are displayed in red, white, and blue, respectively. (*B*) A schematic representation of the modular makeup of cell-permeable TAT-GIV-CT peptides is shown. TAT peptide transduction domain (TAT-PTD) was fused to His and HA tags, and coupled, via a linker (7 residues), to the C terminus of GIV (1660–1870 residues). A GEF-deficient mutant TAT-GIV-CT was generated by substituting a Phe-1685 into an Ala (F1685A). (*C* and *D*) Expression and purification of bacterially expressed TAT-GIV CT peptides. The purity and size of TAT-GIV-CT was confirmed by coomassie staining (*C*) and by immunoblotting (*D*) with anti-His and anti-GIV-CT antibodies.

Gi (7), and (*ii*) a newly defined ∼110-aa stretch that folds into a SH2-like domain in the presence of phosphotyrosine ligands; the latter is necessary and sufficient to recognize and bind specific sites of autophosphorylation on the receptor tail (9, 24). Thus, GIV serves as a platform that links RTKs to G proteins within RTK-GIV-Gαi ternary complexes only when both its GEF and SH2-like modules are intact. In the absence of either of these modules, ligand-activated RTKs and Gαi are uncoupled, and the recruitment of Gαi to RTKs and subsequent activation of G proteins is impaired.

Although the discovery of coexisting SH2-like and GEF modules in-tandem within GIV-CT supported the idea that GIV's C terminus has the necessary modular make-up to serve as a platform for convergent signaling downstream of multiple RTKs via G proteins, it was not possible to visualize this platform until recently, when we developed genetically encoded fluorescent biosensors comprised of these two modules within GIV-CT. These biosensors revealed that the evolutionarily conserved C terminus of GIV represents the smallest, functionally autonomous unit that retains most key properties of full length GIV (25), i.e. (*i*) they can bind and activate Gαi in cells in a GEF dependent manner; (*ii*) they retain the properties of receptor recruitment and signal transduction characteristic of full length GIV; (*iii*) they serve as a bona fide platform for assembly of RTK-Gαi complexes at the PM and for noncanonical activation of Gαi in response to growth factors; and (*iv*) they are sufficient to trigger cell migration/invasion through basement membrane matrix. Thus, comprised of the essential modules (GEF and SH2-like domains), GIV-CT is sufficient for linking G proteins to RTKs, for triggering G protein activation in the vicinity of ligand-activated RTKs, for modulation of growth factor signaling, and for triggering complex cellular processes like cell invasion.

Despite the emergence of GIV-CT as the long-sought platform for noncanonical transactivation of G proteins by multiple growth factor RTKs, exogenous manipulation of this platform has remained out of reach. We have developed cell-permeable

GIV-CT peptides based on the blueprint of the previously extensively characterized fluorescent GIV-CT biosensors (25), and used them successfully to manipulate the diverse pathophysiologic processes in which GIV has been previously implicated. These findings help validate cell-permeable GIV-CT as a versatile tool for exogenously and selectively engineering noncanonical activation of G proteins in response to growth factors.

Results and Discussion

Generation of Cell-Permeable Peptides Comprised of Key Modules Derived from GIV. To generate the cell-permeable peptides, we followed our previously validated strategy of building the multimodular fluorescent GIV biosensors (25). Because TAT-tags provide a reliable means for direct protein transduction into the cell, without inducing toxicity or cell death (26–28), we generated the cell-permeable peptides by fusing the C terminus of GIV (1,660–1,870 residues) at its N terminus with the TAT peptide transduction domain (TAT-PTD) (Fig. 1*B*). A previously described GEF-deficient F1685A mutant (7), henceforth referred to as FA (TAT-GIV-CT-FA), was created to selectively disrupt the GIV-Gαi interaction. A linker was placed between TAT and GIV to allow for flexibility. The constructs also featured a hexa-Histidine (6× His) tag to allow for affinity purification and a Hemagglutinin (HA) tag to allow detection in cells. The rationale for the design of these peptides is multifactorial: (*i*) a complete phylogenetic analysis of GIV (17) has revealed that this stretch of GIV's C terminus could be functionally autonomous because it evolved independently of its N terminus (in fish), and both *N*- and C-termini fused into full length GIV only in birds; (*ii*) the C terminus contains the GEF and SH2-like domains (Fig. 1*B*), representing the cross-road between GPCR/G and RTK signaling pathways; (*iii*) the C terminus of GIV also contains the two critical tyrosines (Y1764 and Y1798) that serve as docking sites for p85α(PI3K) (29); (*iv*) the coexistence of those tyrosines, the GEF motif, and the SH2-like domain is restricted only to the most complex of eukaryotes, i.e., mammals, and is highly conserved (~99%) (17, 29); (*v*) biochemical and functional assays (9, 25) have convincingly demonstrated that the critical C-terminal domain is necessary and sufficient for GIV to carry out its functions during signal transduction downstream of RTKs; and finally, (*vi*) biophysical studies (25) have revealed that fluorescent GIV-CT biosensors are effective tools for visualization and manipulation of the fundamental function of GIV in signal transduction, i.e., enabling dynamic association of Gαi with RTKs and noncanonical transactivation of G proteins in cells responding to growth factors. We expressed and purified (~95–99% purity) the TAT-GIV-CT peptides and confirmed that they were expressed as proteins of expected size by immunoblotting (Fig. 1 *C* and *D*). We hypothesized that these recombinant peptides have the minimal modules that will allow these peptides to induce macropinocytosis and facilitate endosomal escape to enter cytoplasm, and to operate autonomously and carry out most functions that have been previously attributed to the extensively characterized fluorescent GIV-CT biosensors (25) and to full length GIV (reviewed in ref. 17).

Cell-Permeable GIV-CT Peptides Are Effective in Exogenous Modulation of Gi and EGFR Signaling. We carried out several biochemical and functional assays to determine whether TAT-GIV-CT peptides are indeed functional. First, we assessed the ability of TAT-GIV-CT peptides to bind Gαi in vitro. Consistent with the known binding properties of GEFs, TAT-GIV-CT-WT bound inactive (i.e., GDP-loaded) GST-Gαi3 (Fig. 2*A*). As anticipated, the GEF-deficient TAT-GIV-CT-FA peptide did not bind Gαi3 (Fig. 2*A*). Using a GST-tagged GIV-CT peptide (identical length as TAT-GIV-CT peptide) we confirmed that Gαi3 binds GIV with submicromolar affinity [equilibrium dissociation constant (K_d) = 0.24 ± 0.03 μM] (Fig. S2). To analyze the effects of TAT-GIV-CT peptide on cells, we first optimized cellular uptake of these peptides in HeLa cells. We chose to study HeLa cells because this is a well accepted model system and has been extensively used to characterize the role of GIV in our prior work (16, 18, 29, 30). Incubation of HeLa cells with 400–800 nM TAT-GIV-CT peptides for 30 min resulted in efficient uptake (~90–100% cells by immunofluorescence) with no observed toxicity (Fig. 2*B*). Consistent with the central role of GIV's GEF function in actin remodeling (7), transduction of TAT-GIV-CT-WT triggered actin remodeling (as determined by the abundance of actin stress fibers; Fig. 2*B*). By contrast, transduction of the TAT-GIV-CT-FA mutant suppressed stress fibers, and instead enhanced the thickness of cortical actin, identical to the observed pattern of actin cytoskeleton endogenously modulated by full length GIV-FA mutant (7). Next we asked whether TAT-GIV-CT peptides can modulate Gi and epidermal growth factor (EGF) signaling in HeLa cells. We chose to study responses to EGF because it is the ligand for EGF receptor (EGFR), the prototype member of the RTK superfamily, because EGF has been extensively used by us and others to study the cellular functions of GIV (8, 9, 25), and because the structural basis for GIV's interaction with EGFR is most well understood (24). To determine whether TAT-GIV-CT peptides can exogenously modulate Gi activation downstream of EGFR, we used a previously validated assay in which activation of Gi is monitored by dissociation of fluorescently tagged Gαi and Gβγ subunits with a resultant loss of Förster Resonance Energy Transfer (FRET) (31–33). To ensure that the observed changes in FRET are not due to a dominant negative effect of TAT-GIV-CT transduction and to minimize any potential interference posed by endogenous full length GIV, we carried out these assays in HeLa cells depleted of endogenous GIV by shRNA (Fig. S3). As anticipated, when GIV-depleted HeLa cells coexpressing Gαi1-YFP (internal tag), CFP-$Gβ_1$ (N-terminal tag), and $Gγ_2$ (untagged) were stimulated with EGF, no significant loss of FRET was observed, i.e., Gi heterotrimer did not dissociate into Gαi-YFP and CFP-Gβγ subunits at the PM within 5 min (Fig. 2*D* and Fig. S4 *A* and *B*), indicating that EGF fails to trigger Gi activation in the absence of GIV. When these cells were transduced with TAT-GIV-CT-WT, a significant loss of FRET was observed (from 0.22 ± 0.04–0.15 ± 0.07; P = 0.0011) in response to EGF. Similar loss of FRET was not observed when cells were transduced with TAT-GIV-CT-FA peptides (Fig. 2 *C* and *D*), indicating that Gi heterotrimers remained intact at the PM regardless of EGF stimulation, and that Gαi remained inactive. These results demonstrate that TAT-GIV-CT peptides are effective in exogenous modulation of Gi activity downstream of EGFR, i.e., they can bind and activate Gαi and release Gβγ in cells in a GEF-dependent manner as previously demonstrated for full length GIV (7) and fluorescent GIV-CT biosensors (25). These findings also suggest that the TAT-GIV-CT-WT peptides bind Gαi in cells with high affinity that is sufficient to overcome the high affinity that Gβγ-heterodimers have for Gαi•GDP (dissociation constant = ~3–10 nM; ref. 34).

Consistent with the central role of GIV's GEF function in the enhancement of EGFR autophosphorylation (9, 30) and PI3K-Akt signaling downstream (7, 29), transduction with TAT-GIV-CT-FA inhibited receptor autophosphorylation (as determined by phosphorylation at Y1068 and Y1173 on EGFR tail; ref. Fig. 2*E*) and Akt signaling (as determined by the extent of phosphorylation of Akt at Ser-473; Fig. 2*F*). These findings demonstrate that the TAT-GIV-CT biosensors can exogenously modulate EGF signaling characteristic of full length GIV (7, 9, 29, 30) and fluorescent GIV-CT biosensors (25). Taken together, we conclude that TAT-GIV-CT peptides represent the smallest, functionally autonomous units that effectively combine the cell-permeant properties of TAT to exogenously engineer many key signaling properties of GIV in cells.

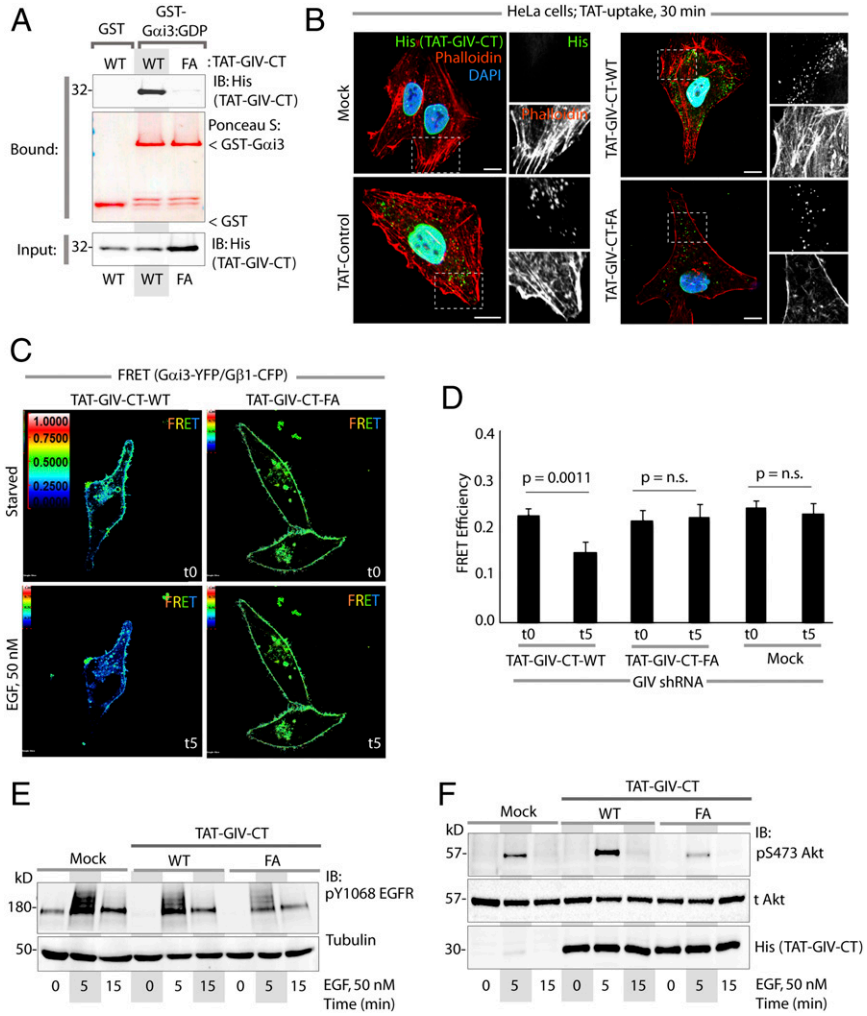

Fig. 2. Cell-permeable TAT-GIV-CT peptides can bind and activate Gi, remodel cytoskeleton and enhance EGF signaling. (*A*) Pulldown assays were carried out with recombinant TAT-GIV-CT-WT or FA proteins and GST-Gαi3 (GDP loaded) immobilized on glutathione beads. Bound (*Upper*) and input (*Lower*) proteins were analyzed for TAT-GIV-CT proteins by immunoblotting with His mAb. WT, but not FA peptides bind Gαi3. (*B*) Monolayers of HeLa cells were transduced with either vehicle (mock) or ∼400 nM TAT-control or TAT-GIV-CT peptides, fixed and costained with phalloidin-Texas red (F-actin, red), DAPI (DNA, blue), anti-His antibody (TAT-GIV-CT, green) and analyzed by confocal microscopy. TAT-GIV-CT-FA, but not WT peptides suppressed the formation of actin stress fibers. Red and green channels of the boxed areas on left are magnified and displayed in grayscale on the right. Bar = 10 μm. (*C* and *D*) HeLa cells depleted of endogenous GIV (by ∼85%; Fig. S3) were cotransfected with Gαi1-intYFP, Gβ1-CFP and untagged Gγ2 were serum starved, transduced with TAT-GIV-CT WT or FA peptides, or vehicle (mock) and then stimulated with 50 nM EGF for 5 min. Cells were analyzed for changes in FRET by confocal live-cell microscopy. Representative freeze-frame images (*C*) are shown, which display intensities of acceptor emission due to FRET in each pixel. Loss of FRET at the plasma membrane (PM) indicate dissociation of trimeric Gi1 (Fig. S4*A*) due to transactivation of G protein exclusively after ligand stimulation (compare t0 and t5 images in cells transduced with TAT-GIV-CT WT). (*D*) Bar graphs display EGF-triggered changes in FRET intensities observed in (*C*). Error bars represent mean ± S.E.M of 5–6 randomly chosen ROIs at the PM per cell, from 4–5 cells per experiment, from six independent experiments. Individual YFP and CFP panels and representative region of interest (ROI) used in the analysis is shown in Fig. S4*B*. (*E* and *F*) HeLa cells were starved and transduced with TAT peptides and stimulated with EGF as in *C* before lysis. Equal aliquots of lysates were analyzed for activation of EGFR (autophoshorylation) was monitored using anti-phospho (p)Y1068 (*E*) and Akt signaling using an anti-phospho (p)Ser473 (*F*) by immunoblotting (IB). TAT-GIV-CT-WT enhances and TAT-GIV-CT-FA suppresses EGFR autophosphorylation and Akt signaling.

Cell-Permeable GIV-CT Proteins Allow Manipulation of a Diverse Array of Complex GIV-Dependent Cellular Processes. Next we asked whether TAT-GIV-CT peptides can exogenously modulate complex, multireceptor driven cellular phenotypes previously attributed to full length GIV, e.g., cell migration (8, 9) (Fig. 3 *A*–*C*) and tumor cell invasion through basement membrane during cancer metastasis (10) (Fig. 3 *D*–*F*). To determine whether TAT-GIV-CT peptides affect 2D-cell migration, we carried out scratch-wound assays on confluent monolayers of HeLa cells transduced with TAT proteins (Fig. 3*A*). We found that, compared with mock treatment, TAT-GIV-CT-WT peptides enhanced 2D-migration and wound closure more efficiently, whereas the FA mutant peptides delayed wound closure (Fig. 3*B*). Consistent with the enhancement or delay in wound closure, EGFR autophosphorylation and Akt activation were enhanced in WT but not in FA-transduced cells (Fig. 3*C*). These results demonstrate that TAT-GIV-CT peptides are capable of exogenously modulating 2D-cell migration, and the key PI3K-Akt signaling pathway that drives such migration.

Next we analyzed the effect of TAT-GIV-CT peptides on cancer cell invasion through polypropylene membranes that are precoated with basement membrane protein in a 3D Transwell assay (Fig. 3 *D*–*F*). We used the highly invasive MDA MB231 triple negative breast cancer cell lines that are not only known to express GIV at very high levels (8, 9, 18, 23) but also require GIV

for metastatic progression in murine models (10) (Fig. 3*D*). Invasion of MDA MB231 cells through the basement membrane matrix in response to an EGF gradient was significantly enhanced when cells were pretreated with TAT-GIV-CT-WT peptides compared with cells transduced with TAT-control peptides (Fig. 3 *E* and *F*). By contrast, invasion was virtually

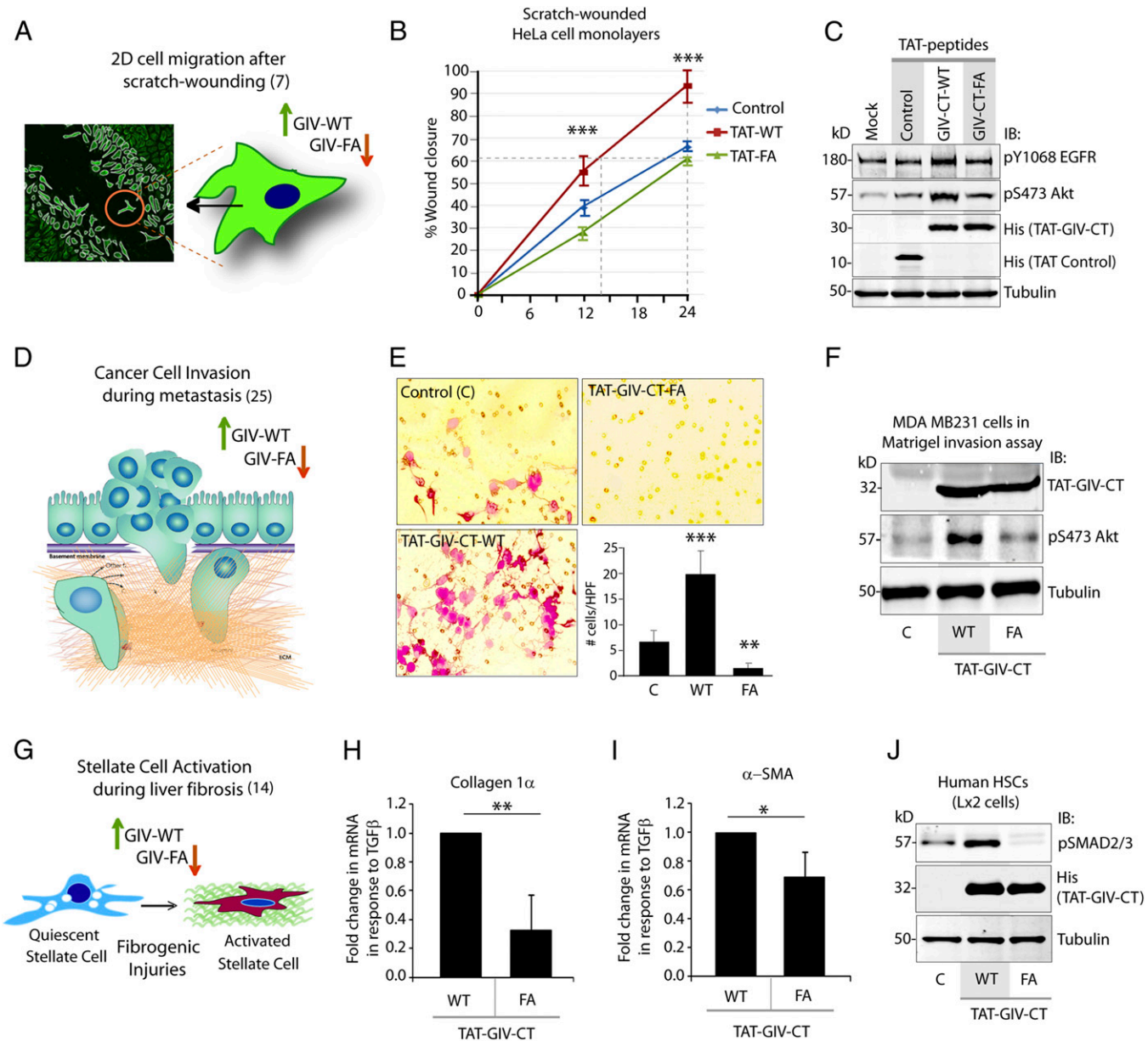

Fig. 3. TAT-GIV-CT proteins can effectively manipulate a diverse array of GIV-dependent pathophysiologic processes. (*A*) A schematic summarizing the opposing effect of GIV-WT (enhancement) and GIV-FA (suppression) on scratch-wound induced cell migration in 2D (7). (*B*) Confluent monolayers of HeLa cells were transduced with TAT peptides, scratch-wounded, and assessed for wound closure by serial imaging of the wound for 12 h and 24 h. Graphs display the quantification of % wound area closed by 12 h and 24 h, expressed as migration index (*y* axis). TAT-GIV-CT-WT, but not FA enhances 2D cell migration. ***$P < 0.001$. (*C*) Whole cell lysates of HeLa cells treated as in *B* and harvested at 6 h postwounding were analyzed for activation of EGFR and Akt signaling pathway by immunoblotting (IB) exactly as in Fig. 2 *E* and *F*. TAT-GIV-CT-WT, but not FA enhances EGFR autophosphorylation and Akt signaling during 2D cell migration. (*D*) A schematic summarizing the opposing effect of GIV-WT (enhancement) and GIV-FA (suppression) on tumor cell invasion through basement membrane (25). (*E*) MDA MB231 cells transduced with TAT peptides were analyzed for their ability to invade transwell membranes coated with Matrigel in response to EGF. Images display a representative field of the matrigel-coated membrane insert showing crystal violet-stained cells (purple) that have successfully invaded. Bar graphs show quantification of the number of invasive cells/HPF. Error bars represent mean ± SD of each TAT construct per transwell, from three independent experiments. *P* values for statistical comparison with control are displayed; ***$P < 0.001$ and **$P < 0.01$. (*F*) Equal aliquots of MDA MB231 cells transduced with TAT-peptides in *E* were analyzed for TAT uptake and Akt signaling by immunoblotting. (*G*) A schematic summarizing the opposing effect of GIV-WT (enhancement) and GIV-FA (suppression) on HSC activation and collagen production (14). (*H-J*) Serum-starved Lx2 cells were treated with TGFβ1 for 24 h while simultaneously being serially transduced with TAT peptides every 8 h. Cells were analyzed for Collagen α1 (*H*) and α-SMA (*I*) by qPCR. Results are displayed as fold change in response to TGFβ1 (*y* axis). Values are normalized to the fold change observed in control cells. Error bars represent mean ± SD; $n = 3$; **$P < 0.01$ for collagen and *$P < 0.05$ for αSMA. (*J*) Equal aliquots of lysates of TAT-transduced Lx2 cells were analyzed for the uptake of TAT-GIV-CT proteins and phosphorylation of SMAD2/3 by immunoblotting (IB).

abolished by the TAT-GIV-CT-FA mutant peptide. Taken together, these findings indicate that TAT-GIV-CT-WT peptide is sufficient to enhance both epithelial cell migration in 2D after wounding and tumor cell invasion through the basement membrane matrix in 3D, and that peptides that lack a functionally intact GEF motif (i.e., FA) can exert a dominant negative effect and effectively inhibit both processes.

Next we asked whether the cell-permeable GIV peptides can modulate another recently defined function of GIV, i.e., activation of myofibroblasts and collagen synthesis in response to chronic injuries (14) (Fig. 3 *G–J*). Using myofibroblasts of the liver (i.e., human hepatic stellate cells; HSCs) as a model system, we recently showed that GIV's C terminus serves as a central hub within the signaling network initiated by TGFβR, PDGFR and other diverse classes of fibrogenic receptors. GIV triggers HSC activation by skewing the signaling network in favor of fibrosis, i.e., enhances the profibrotic (PI3K-Akt-FoxO1 and TGFβ-SMAD) and inhibits the anti-fibrotic (cAMP-PKA-pCREB) pathways, all via activation of Gαi (Fig. 3*G*). We asked whether HSC activation in response to TGFβ can be suppressed by GEF-deficient GIV-CT peptides. We found that compared with control cultured human HSCs (Lx2 cells) and HSCs transduced with TAT-GIV-CT-WT, transduction with TAT-GIV-CT-FA suppressed collagen production by ∼70% (Fig. 3*H*) and reduced HSC activation by ∼30%, as determined by α-SMA expression levels (Fig. 3*I*). These changes in fibrogenic phenotypes were accompanied by an underlying suppression of the profibrogenic TGFβ-SMAD cascade, as determined by phosphorylation of SMAD2/3 (Fig. 3*J*). We conclude that cell-permeable GIV-CT-FA peptides that lack a functional GEF motif are sufficient for inhibition of TGFβ- triggered activation of HSCs. These findings also demonstrate that TAT-GIV-CT peptides can effectively modulate multireceptor driven Gi signaling in HSCs.

Taken together, we conclude that cell-permeable GIV-CT peptides represent a versatile strategy to modulate various growth factor responses, in diverse cell types, to modulate a wide array of cellular processes driven by GIV-GEF.

Cell-Permeable GIV-CT-WT Peptides Accelerate Wound Healing in Mice. Next we analyzed the therapeutic potential of TAT-GIV-CT peptides in vivo in the modulation of the complex, multireceptor-driven process of dermal wound-healing in mice. The rationale for our choice to study wound healing was multifactorial. First, wound healing is a multireceptor-driven process that involves coordination of diverse cell populations and cellular processes. Second, the ubiquitous expression of GIV in all cell types involved in healing, the transcriptional up-regulation of GIV after wounding, and the role GIV-GEF in many of those cells/processes has been well documented (7, 8, 11, 13, 14, 17, 18, 22, 35) (Fig. 4*A*). Third, a variety of growth factors and their corresponding RTKs trigger wound closure, and GIV has been shown to bind and modulate signal transduction downstream of many of those RTKs (see Fig. 4*A*). Finally, wound healing remains a challenging clinical problem, and the development of new therapeutic approaches and technologies is critical. Of the many pathophysiologic processes modulated by TAT-GIV-CT (Fig. 3), its topical application on wounds is the most feasible therapeutic application. We made full-thickness 6 mm punch biopsy wounds on the dorsum of mice, treated them with 500 pmol TAT-GIV-CT (WT and FA) or TAT control peptides daily, and compared their rates of healing in blinded manner (Fig. 4*B*). Compared with TAT-treated controls, the treatment group exposed to TAT-GIV-CT-WT demonstrated accelerated wound healing (∼2× the rate and a day earlier), whereas the group treated with the FA mutant demonstrated delayed wound healing (Fig. 4 *C* and *D*). These findings demonstrate that topical application of TAT-GIV-CT peptides accelerate wound healing, and that the GEF motif is critical for this observed therapeutic effect. We conclude that cell-permeable GIV-CT peptides retain their functionality in vivo, and are capable of modulating complex multicellular pathophysiologic processes.

Conclusion

Here we presented the rationale, validation, and effectiveness of a nongenetic technique for manipulating an emerging signaling pathway/paradigm, i.e., transactivation of Gαi subunits by growth factors via the GIV platform. The TAT-GIV-CT peptides we describe here were designed to retain two fundamental properties of full-length GIV: activate Gαi by enhancing nucleotide release via its GEF motif and interact with ligand-activated RTKs via its SH2-like motif. We determined that appending a TAT leader sequence was able to make the GIV-CT peptide cell permeable without altering either of those properties. Our findings also demonstrate that TAT-GIV-CT peptides may, more generally, be used as a versatile strategy to assemble RTK-Gαi complexes in diverse cell types and trigger activation of Gi downstream of a variety of growth factors. By the same token, the dominant negative GEF-deficient mutant FA peptides, which inhibit the formation of RTK-Gαi complexes, offer a strategy for inhibiting aberrant signaling via this pathway. Thus, TAT-GIV-CT-WT serves as a peptide agonist that enhances the RTK-Gi pathway for G protein activation, whereas the FA mutant peptide antagonizes it.

The impact of our findings is twofold. First, it firms up an emerging hypothesis which challenges the long-held tenet that heterotrimeric G proteins are activated exclusively by GPCRs. Our recent work has revealed that RTKs can indeed interact with and activate Gαi (30) during a variety of pathophysiologic processes (7, 14, 21) using the C terminus of GIV as a platform for such RTK-G protein cross-talk (25). The findings described here using TAT-GIV-CT peptides represent a significant advancement in our ability to access, interrogate and manipulate that platform, and thereby, modulate the cross-talk it facilitates. Second, G proteins are an ideal target for therapeutic intervention because they serve as signal amplification switches, and potent and pathway-selective activators/inhibitors of a G protein can serve multiple purposes ranging from being a research tool to pharmacologic probe for use in experimental and clinical therapeutics (36). The technique we define here allows exogenous manipulation of the RTK-GIV-Gi pathway by enhancing or suppressing the coupling of G protein with RTKs and their subsequent transactivation, in a dose-dependent manner while minimizing the risk of tampering with other physiologic functions/interactions of G proteins/or other components within the network of modulators of G protein signaling (37).

The therapeutic advantages of using cell-permeable GIV-CT peptides for activation/inactivation of Gαi are also many-fold. First, their use circumvents the need to target individual receptors in diseases that are driven by multiple receptors. Second, GIV's SH2-like domain can directly bind multiple ligand-activated RTKs and rewire several components of downstream signaling (Fig. S1), and therefore, these peptides offer a versatile tool to simultaneously modulate multiple pathways downstream of many RTKs (i.e., broad), even in diseases/processes where upstream and downstream events are incompletely understood (i.e., circumvents the limitations of unknown). Third, because GIV binds preferentially to Gi subfamily members but can discriminate within this subfamily by binding to Gαi subunits but not to the close homolog Gαo (∼75% overall similarity to Gαi1/2/3 subunits) (38), TAT-GIV-CT peptides selectively affect the activation of Gαi1/2/3, but not Gαo (i.e., specific). Fourth, these peptides circumvent the limitation that no promising "druggable" pockets have been identified within GIV's C terminus, and that small molecules that can selectively block this platform are yet to be identified. Last, these GIV-CT peptides are predicted to directly address the upstream component of RTK-related signaling in cases

of mutations, polymorphisms, and expression-related defects often seen in disease.

In conclusion, we have developed cell-permeable peptides that allow exogenous modulation of the fundamental function of GIV, i.e., activate Gi downstream of growth factor RTKs. These peptides provide a versatile tool to manipulate Gαi activation downstream of multiple growth factors in different cell types and in a diverse array of pathophysiologic conditions. The therapeutic potential of these peptides is expected to grow with the rapidly growing list of pathophysiologic processes that GIV modulates.

Experimental Procedures

A detailed description of all of the experimental procedures can be found in *SI Experimental Procedures*.

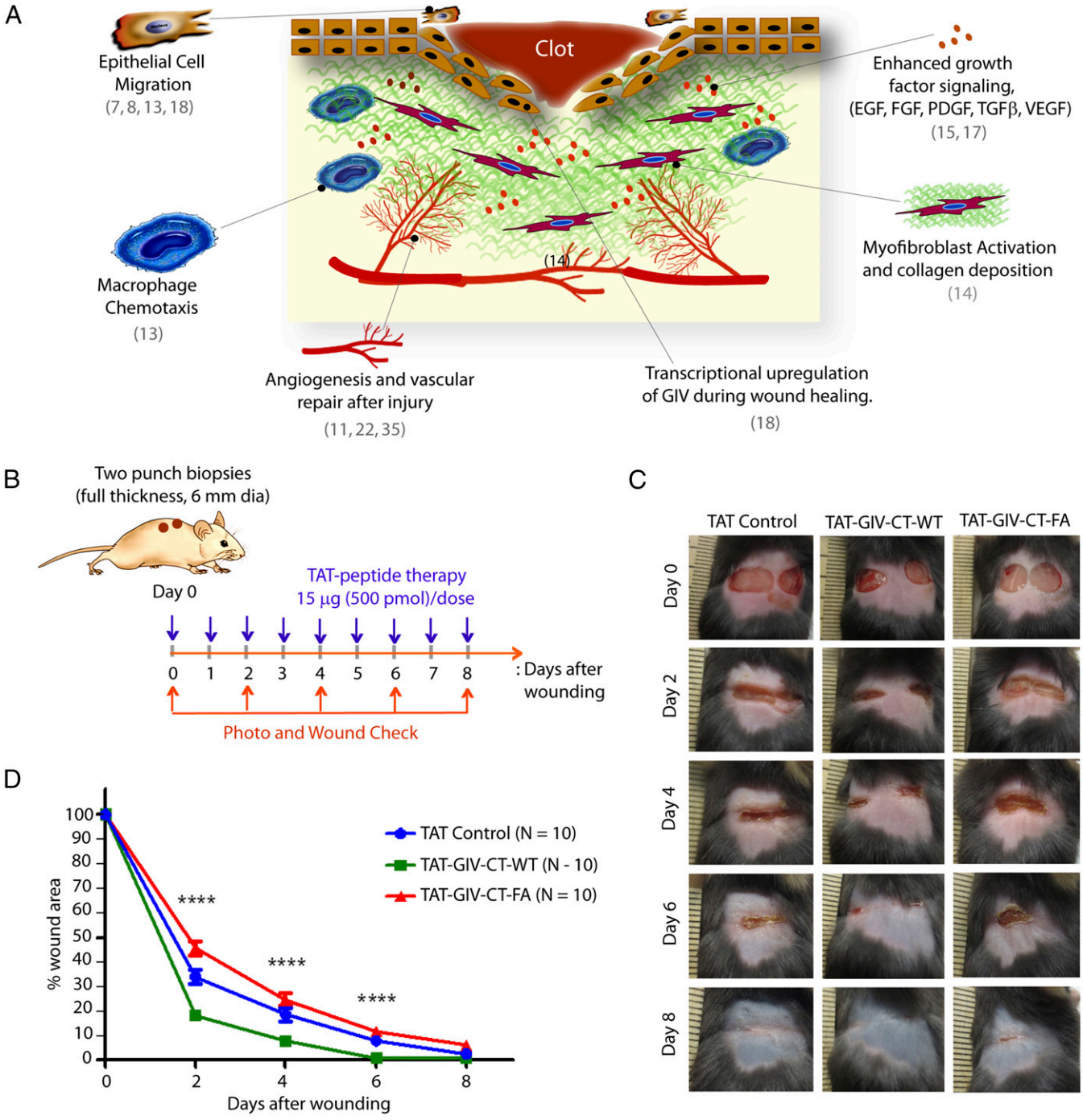

Fig. 4. Topical application of cell-permeable GIV-CT-WT peptides accelerate dermal wound healing. (*A*) A schematic summarizing GIV's role in modulating functions of a variety of cell types that trigger key aspects of tissue response after wounding (7, 8, 11, 13–15, 17, 18, 22, 35), all of which coordinately facilitate wound healing. The supporting literature is cited in each context. (*B*) Schematic showing the randomized blinded study protocol for dermal wound healing in mice. Two punch biopsy wounds per mice made on day 0 were treated with 15 μg (~500 pmol) TAT proteins every 24 h for 8 d. $n = 10$ wounds per treatment arm. (*C*) Representative photographs of wounds obtained every 48 h from each treatment arm are displayed. (*D*) Graphs show quantification of % wound area (*y* axis) at various times. Compared with TAT-control, TAT-GIV-CT-WT accelerates and FA retards wound healing. Error bars represent mean ± SD ****$P < 0.0001$.

TAT-Protein Expression and Purification. Cloning of TAT-GIV-CT was carried out by amplifying a short flexible linker (Fig. 1*A*) and the stretch of human GIV-CT (aa 1660–1870) *en bloc* from CFP-GIV-CT (25) and inserting it between *Nco*1/*Kpn*1 of pTAT-HA. TAT-GIV-CT-FA mutant was generated using QuikChange II (Stratagene) and specific primers (sequence available upon request) following the manufacturer´s instructions. TAT-constructs were expressed using BL21(DE3)-pLysS (Invitrogen) and Terrific Broth (BioPioneer) supplemented with additives as per auto-induction protocols outlined by Studier F (39). Briefly, cultures of bacteria were grown at 300 rpm at 37°C for 5 h, then at 25°C overnight. Cells were lysed in 10 mL of buffer [20 mM Tris, 10 mM Imidazole, 400 mM NaCl, 1% (vol:vol) Sarkosyl, 1% (vol:vol) Triton X-100, 2 mM DTT, 2 mM Na3oV4 and protease inhibitor mixture (Roche Diagnostics) (pH 7.4)], sonicated (3×30 s), cleared at $12{,}000 \times g$ for 20 min at 4°C and affinity-purified on Ni-NTA agarose resin (Quiagen) (4 h at 4 °C). Proteins were eluted in elution buffer [20 mM Tris, 300 mM Imidazole, 400 mM NaCl, pH 7.4], dialyzed overnight against TBS containing 400 mM NaCl and stored at −80 °C.

TAT-Protein Transduction. For TAT-protein transduction, cells were incubated with 400–800 nM of the TAT-proteins for 30 min at 37 °C before three washes with PBS and addition of fresh growth media. For analysis of EGF signaling, subconfluent monolayers of HeLa cells were treated with TAT proteins for 30 min, washed with PBS, and subsequently stimulated with EGF (50 nM) at 4 h after TAT transduction. For scratch-wound assays, HeLa monolayers were treated with TAT proteins before and at 12 h after wounding. For cancer cell invasion assays, highly invasive MDA MB 231 breast cancer cells were plated in six-well dishes, treated with TAT-peptides for 30 min and subsequently lifted and placed in transwell chamber in the presence of serum-free media. For Lx2 myofibroblast activation assays, cells were first treated with TAT-proteins for 30 min, starved in serum-free media, and subsequently treated with 1.5 ng/mL TGF-β for 24 h. TAT-protein transduction was repeated every 8 h during the course of TGFβ stimulation (total 3 treatments). In each case, whole cell lysates prepared from cells in duplicate wells were analyzed for signaling pathways and TAT-protein uptake by immunoblotting.

FRET Studies. HeLa cells stably depleted of GIV by shRNA were grown to 60–70% confluence in sterile 35-mm MatTek glass bottom dishes. One microgram each of various donor and acceptor plasmid constructs were transfected with Trans-IT-LT1 tansfection reagent (Mirus Bio LLC) using manufacturer's protocol. Cells were starved overnight in serum-free DMEM (Gibco), transduced the following morning with TAT proteins for 30 min, washed with PBS and subsequently the media was switched to DMEM without phenol red before live cell imaging. EGF stimulation was carried out ∼4 h after TAT transduction. Fluorescence microscopy studies were conducted on single cells in mesoscopic regime to avoid inhomogeneities from samples as rationalized by Midde et al. (40–42). Olympus FV1000 inverted confocal laser scanning microscope was used for live cell FRET imaging (UCSD-Neuroscience core facility). Details on how cells were chosen and analyzed, microscopy technique and controls used to correct for cross-talk, background, autofluorescence, and light scattering are provided in *SI Experimental Procedures*.

Scratch-Wounding and Migration Index. Scratch-wound assays were done as described (13). Briefly, monolayer cultures (100% confluent) of HeLa cells were incubated first in a 0.2% serum media overnight. The following morning, monolayers of HeLa cells were first transduced with TAT peptides for 30 min, then washed three times with PBS and placed again in a 0.2% serum media for 1 h 30 min before scratch-wounding. Transduction with TAT peptides was repeated at 12 h into the wound healing assay (a total of two times). Healing wounds were monitored by phase-contrast microscopy over the next 24 h, and migration index was quantified (expressed as % wound closure) by measuring the wounded area using Image J software.

Tumor Cell Invasion Assays. Invasion assays were performed using Corning Transwell plates according to the manufacturer's protocol. Transduced cells were trypsinized, counted, and placed in a Corning transwell permeable support coated with Cultrex Basement Membrane Extract (7×10^4 cells per well). Media without FBS but containing EGF ligand (50nM) was placed within the bottom chamber of each well to trigger directional 3D invasion. trandsuction with TAT peptides was repeated one more time ∼10–12 h into the assay (total of two times). Cells that had successfully invaded to the side of the permeable membrane facing the bottom chamber were visualized by staining the membrane with crystal violet. Cell invasion (expressed as number of invasive cells/high power field) was quantified by analyzing ∼10–12 random fields per membrane insert per condition for number of crystal violet stained cells.

RNA Isolation and Quantitative PCR. For measurement of collagen and αSMA mRNA levels in Lx2 HSCs we followed the protocols exactly as before (14).

Dermal Wound Healing in Mice. Under general anesthesia, two 6-mm-diameter punch biopsy wounds were created on the shaved dorsal surface of 8 wk old female *C56BL*/6 wild-type mice under sterile conditions. Wounds were then treated with TAT proteins every 24 h, and photographed every 48 h over 8 d after injury, and wound area was measured by manual tracing (*SI Experimental Procedures*) and analyzed using Image J (NIH) software. Five mice, each with 2 wounds (a total of 10 wounds) were studied in each treatment arm. These studies were carried out in a blinded manner.

Data Analysis and Other Methods. All experiments were repeated at least three times, and results were presented either as one representative experiment or as average ± SD or SEM. Statistical significance was assessed with the Student's *t* test. $^{*}P < 0.05$; $^{**}P < 0.01$; $^{***}P < 0.001$; $^{****}P < 0.0001$. Protein structure analysis and visualization were performed using ICM Browser Pro software (Molsoft).

ACKNOWLEDGMENTS. We thank Steven Dowdy, Marilyn Farquhar, Gordon Gill, and Mehul Shah (UCSD) for thoughtful comments along the way and during the preparation of this manuscript. This work was funded by NIH Grants R01 CA160911 and DK099226, American Cancer Society (IRG #70-002), and the Burroughs Wellcome Fund (CAMS award) (to P.G.). R.L.G. was supported by NIH Grants R01AI052453, AR052728, and P01HL107150; G.S.M was supported by the Doris Duke Charitable Foundation (DDCF Grant 2013073; to P.G.); I.L.-S. was supported by the American Heart Association (AHA 14POST20050025); N.K. was supported by a predoctoral fellowship from the NCI (T32CA067754) and K.K.M. was supported by a fellowship from the Susan G. Komen Foundation (SGK PDF14298952). Live cell microscopy facilities were supported in part by University of California, San Diego, Neuroscience Microscopy Shared Facility Grant P30 NS047101.

1. Schlessinger J (2014) Receptor tyrosine kinases: Legacy of the first two decades. *Cold Spring Harb Perspect Biol* 6(3).
2. Gilman AG (1987) G proteins: Transducers of receptor-generated signals. *Annu Rev Biochem* 56:615–649.
3. Daub H, Weiss FU, Wallasch C, Ullrich A (1996) Role of transactivation of the EGF receptor in signalling by G-protein-coupled receptors. *Nature* 379(6565):557–560.
4. Natarajan K, Berk BC (2006) Crosstalk coregulation mechanisms of G protein-coupled receptors and receptor tyrosine kinases. *Methods Mol Biol* 332:51–77.
5. Pierce KL, Luttrell LM, Lefkowitz RJ (2001) New mechanisms in heptahelical receptor signaling to mitogen activated protein kinase cascades. *Oncogene* 20(13):1532–1539.
6. Marty C, Ye RD (2010) Heterotrimeric G protein signaling outside the realm of seven transmembrane domain receptors. *Mol Pharmacol* 78(1):12–18.
7. Garcia-Marcos M, Ghosh P, Farquhar MG (2009) GIV is a nonreceptor GEF for G alpha i with a unique motif that regulates Akt signaling. *Proc Natl Acad Sci USA* 106(9):3178–3183.
8. Enomoto A, et al. (2005) Akt/PKB regulates actin organization and cell motility via Girdin/APE. *Dev Cell* 9(3):389–402.
9. Ghosh P, et al. (2010) A Galphai-GIV molecular complex binds epidermal growth factor receptor and determines whether cells migrate or proliferate. *Mol Biol Cell* 21(13):2338–2354.
10. Jiang P, et al. (2008) An actin-binding protein Girdin regulates the motility of breast cancer cells. *Cancer Res* 68(5):1310–1318.
11. Kitamura T, et al. (2008) Regulation of VEGF-mediated angiogenesis by the Akt/PKB substrate Girdin. *Nat Cell Biol* 10(3):329–337.
12. Garcia-Marcos M, Ear J, Farquhar MG, Ghosh P (2011) A GDI (AGS3) and a GEF (GIV) regulate autophagy by balancing G protein activity and growth factor signals. *Mol Biol Cell* 22(5):673–686.
13. Ghosh P, Garcia-Marcos M, Bornheimer SJ, Farquhar MG (2008) Activation of Galphai3 triggers cell migration via regulation of GIV. *J Cell Biol* 182(2):381–393.
14. Lopez-Sanchez I, et al. (2014) GIV/Girdin is a central hub for profibrogenic signalling networks during liver fibrosis. *Nat Commun* 5:4451.
15. Garcia-Marcos M, Ghosh P, Farquhar MG (2015) GIV/ Girdin transmits signals from multiple receptors by triggering trimeric G protein activation. *J Biol Chem* 290(11):6697–6704.
16. López-Sánchez I, et al. (2013) Protein kinase C-theta (PKCθ) phosphorylates and inhibits the guanine exchange factor, GIV/Girdin. *Proc Natl Acad Sci USA* 110(14):5510–5515.
17. Ghosh P, Garcia-Marcos M, Farquhar MG (2011) GIV/Girdin is a rheostat that fine-tunes growth factor signals during tumor progression. *Cell Adhes Migr* 5(3):237–248.

18. Dunkel Y, et al. (2012) STAT3 protein up-regulates Gα-interacting vesicle-associated protein (GIV)/Girdin expression, and GIV enhances STAT3 activation in a positive feedback loop during wound healing and tumor invasion/metastasis. *J Biol Chem* 287(50):41667–41683.
19. Ohara K, et al. (2012) Involvement of Girdin in the determination of cell polarity during cell migration. *PLoS ONE* 7(5):e36681.
20. Natsume A, et al. (2012) Girdin maintains the stemness of glioblastoma stem cells. *Oncogene* 31(22):2715–2724.
21. Wang HMT, Taupin V, Eguchi A, Ghosh P, Farquhar MG (2014) GIV/Girdin links VEGF signaling to Akt survival signaling in podocytes independent of nephrin. *J Am Soc Nephrol*, in press.
22. Miyake H, et al. (2011) The actin-binding protein Girdin and its Akt-mediated phosphorylation regulate neointima formation after vascular injury. *Circ Res* 108(10): 1170–1179.
23. Garcia-Marcos M, et al. (2011) Expression of GIV/Girdin, a metastasis-related protein, predicts patient survival in colon cancer. *FASEB J* 25(2):590–599.
24. Lin C, et al. (2014) Structural basis for activation of trimeric Gi proteins by multiple growth factor receptors via GIV/Girdin. *Mol Biol Cell* 25(22):3654–3671.
25. Midde KK, et al. (2015) Multimodular biosensors reveal a novel platform for activation of G proteins by growth factor receptors. *Proc Natl Acad Sci USA* 112(9): E937–E946.
26. Becker-Hapak M, Dowdy SF (2003) Protein transduction: generation of full-length transducible proteins using the TAT system. *Curr Protocols Cell Biol*, Chapter 20:Unit 20 22.
27. van den Berg A, Dowdy SF (2011) Protein transduction domain delivery of therapeutic macromolecules. *Curr Opin Biotechnol* 22(6):888–893.
28. Wadia JS, Stan RV, Dowdy SF (2004) Transducible TAT-HA fusogenic peptide enhances escape of TAT-fusion proteins after lipid raft macropinocytosis. *Nat Med* 10(3): 310–315.
29. Lin C, et al. (2011) Tyrosine phosphorylation of the Gα-interacting protein GIV promotes activation of phosphoinositide 3-kinase during cell migration. *Sci Signal* 4(192):ra64.
30. Lin C, et al. (2014) Structural basis for activation of trimeric Gi proteins by multiple growth factor receptors via GIV/Girdin. *Mol Biol Cell* 25(22):3654–3671.
31. Janetopoulos C, Jin T, Devreotes P (2001) Receptor-mediated activation of heterotrimeric G-proteins in living cells. *Science* 291(5512):2408–2411.
32. Gibson SK, Gilman AG (2006) Gialpha and Gbeta subunits both define selectivity of G protein activation by alpha2-adrenergic receptors. *Proc Natl Acad Sci USA* 103(1): 212–217.
33. Bünemann M, Frank M, Lohse MJ (2003) Gi protein activation in intact cells involves subunit rearrangement rather than dissociation. *Proc Natl Acad Sci USA* 100(26): 16077–16082.
34. Sarvazyan NA, Remmers AE, Neubig RR (1998) Determinants of gi1alpha and beta gamma binding. Measuring high affinity interactions in a lipid environment using flow cytometry. *J Biol Chem* 273(14):7934–7940.
35. Ito T, et al. (2013) Girdin and its phosphorylation dynamically regulate neonatal vascular development and pathological neovascularization in the retina. *Am J Pathol* 182(2):586–596.
36. Iiri T, Farfel Z, Bourne HR (1998) G-protein diseases furnish a model for the turn-on switch. *Nature* 394(6688):35–38.
37. Siderovski DP, Willard FS (2005) The GAPs, GEFs, and GDIs of heterotrimeric G-protein alpha subunits. *Int J Biol Sci* 1(2):51–66.
38. Slep KC, et al. (2008) Molecular architecture of Galphao and the structural basis for RGS16-mediated deactivation. *Proc Natl Acad Sci USA* 105(17):6243–6248.
39. Studier FW (2005) Protein production by auto-induction in high density shaking cultures. *Protein Expr Purif* 41(1):207–234.
40. Midde K, et al. (2013) Comparison of orientation and rotational motion of skeletal muscle cross-bridges containing phosphorylated and dephosphorylated myosin regulatory light chain. *J Biol Chem* 288(10):7012–7023.
41. Borejdo J, Rich R, Midde K (2012) Mesoscopic analysis of motion and conformation of cross-bridges. *Biophys Rev* 4(4):299–311.
42. Midde K, et al. (2014) Membrane topology of human presenilin-1 in SK-N-SH cells determined by fluorescence correlation spectroscopy and fluorescent energy transfer. *Cell Biochem Biophys* 70(2):923–932.